Concentrating light in Cu(In,Ga)Se₂ solar cells

Martina Schmid
Guanchao Yin
Min Song
Shengkai Duan
Berit Heidmann
Diego Sancho-Martinez
Steven Kämmer
Tristan Köhler
Phillip Manley
Martha Ch. Lux-Steiner

Concentrating light in Cu(In,Ga)Se₂ solar cells

Martina Schmid,[a,b,]* Guanchao Yin,[a] Min Song,[a,b] Shengkai Duan,[a] Berit Heidmann,[a,b] Diego Sancho-Martinez,[a] Steven Kämmer,[a,b] Tristan Köhler,[a] Phillip Manley,[a] and Martha Ch. Lux-Steiner[b,c]

[a]Helmholtz-Zentrum Berlin, Nanooptische Konzepte für die PV, Berlin, Germany
[b]Freie Universität Berlin, Department of Physics, Berlin, Germany
[c]Helmholtz-Zentrum Berlin, Berlin, Germany

Abstract. Light concentration has proven beneficial for solar cells, most notably for highly efficient but expensive absorber materials using high concentrations and large scale optics. Here, we investigate the light concentration for cost-efficient thin-film solar cells that show nano- or microtextured absorbers. Our absorber material of choice is $Cu(In, Ga)Se_2$ (CIGSe), which has a proven stabilized record efficiency of 22.6% and which—despite being a polycrystalline thin-film material—is very tolerant to environmental influences. Taking a nanoscale approach, we concentrate light in the CIGSe absorber layer by integrating photonic nanostructures made from dielectric materials. The dielectric nanostructures give rise to resonant modes and field localization in their vicinity. Thus, when inserted inside or adjacent to the absorber layer, absorption and efficiency enhancement are observed. In contrast to this internal absorption enhancement, external enhancement is exploited in the microscaled approach: mm-sized lenses can be used to concentrate light onto CIGSe solar cells with lateral dimensions reduced down to the micrometer range. These micro solar cells come with the benefit of improved heat dissipation compared with the large scale concentrators and promise compact high-efficiency devices. Both approaches of light concentration allow for reduction in material consumption by restricting the absorber dimension either vertically (ultrathin absorbers for dielectric nanostructures) or horizontally (microabsorbers for concentrating lenses) and have significant potential for efficiency enhancement. © 2017 Society of Photo-Optical Instrumentation Engineers (SPIE) [DOI: 10.1117/1.JPE.7.018001]

Keywords: chalcopyrite solar cells; CIGSe; ultrathin absorber; nanoparticles; photonics; light concentration; microabsorber; optical modeling.

Paper 16103P received Sep. 26, 2016; accepted for publication Jan. 13, 2017; published online Feb. 8, 2017.

1 Introduction

Thin-film solar cells based on $Cu(In, Ga)Se_2$ (CIGSe) are experiencing an exciting continuous rise in record efficiencies, the current record being 22.6%.[1] This development can be expected to further increase the share of CIGSe solar cells in the photovoltaic market. When envisaging production on the terrawatt scale, however, the price and supply risk of the contained elements indium and gallium may become a limiting factor.[2] Saving the absorber material while maintaining or even increasing the efficiency therefore is a central goal to further foster CIGSe competitiveness.

Aside from the proven high record efficiencies, CIGSe solar cells offer the additional benefit of being very tolerant against environmental factors, such as shading or even cosmic radiation.[3] This ability makes them a natural fit for concepts that offer material saving and efficiency enhancement, but at the same time, perturb the standard growth processes, or involve nonuniform illumination conditions. For material saving purpose, the absorber dimensions can be reduced in two ways: either vertically by decreasing the absorber thickness from the standard
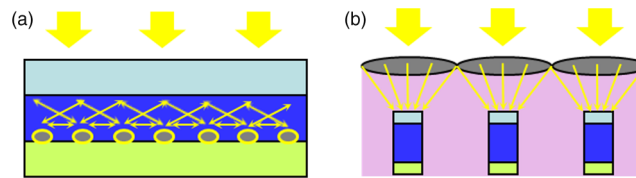

Fig. 1 Concepts for material saving and efficiency enhancement in CIGSe solar cells: (a) ultrathin solar cell with integrated nanostructures for localizing light inside the absorber material, (b) micrometer-sized solar cells under concentrated illumination due to the application of microlenses.

2 to 3 μm to below 500 nm or horizontally depositing spaced out periodically placed absorbers of about 100- to 400-μm diameter. Both cases will initially lead to a loss of incident light due to incomplete absorption in the ultrathin CIGSe or due to light passing in between the locally restricted microabsorbers, respectively. The initial loss of incident sun light needs to be tackled by sophisticated concepts for light localization inside the reduced absorber volume. On the nanoscale, plasmonic and photonic nanostructures are a promising approach to trap light in ultrathin layers by near-field enhancement, large-angle scattering, and coupling into waveguide modes.[4] Absorption enhancement by nanostructures has been proven for various types of photovoltaic devices like silicon or organic solar cells.[5] Recently, we also have delivered the experimental proof of absorption enhancement by dielectric nanostructures in ultrathin CIGSe solar cells.[6,7] Based on this first verification, further development became attractive and offers highly promising improvement. For the microscaled approach, light concentration onto the local absorbers occurs due to microlenses that collect the incident light and focus it onto the small absorbers. Microconcentrator solar cells have equally been demonstrated in the field of silicon photovoltaics,[8] but first investigations of the concept also exist in the area of CIGSe.[9,10] In this paper, we give our latest results for the development of absorption enhancement in ultrathin CIGSe solar cells and light concentration onto micrometer-sized solar cells and highlight both achievements and future challenges. The two concepts of nano- and microscaled light concentration in CIGSe solar cells, which we will discuss in the following, are shown in Figs. 1(a) and 1(b). The blue layer represents the CIGSe absorber deposited on the back contact shown in green, which in the standard configuration is Mo. The light blue part on top combines the window layers consisting of CdS, intrinsic ZnO, and ZnO:Al. Furthermore, in Fig. 1(a) the nanoparticles are depicted leading to near-field enhancement and scattering, and in Fig. 1(b) the concentrator lenses are exemplarily added on top to achieve light focusing.

2 Absorption Enhancement in Ultrathin Solar Cells

In standard CIGSe solar cells, the absorber thickness is chosen as 2 to 3 μm to assure high material quality and complete absorption. Despite this, 1-μm thickness is sufficient, in principle, for complete absorption of photons with energies larger than the band gap. The minimum value of 1000 nm absorber thickness, above which a high performance of CIGSe solar cells can be assured, is a result of optical simulations as well as of experimental investigations.[11] Below 1000 nm thickness, the absorption starts to drop significantly, especially in the long wavelength region, as can also be seen from Fig. 2(a). The measured external quantum efficiency (EQE) of CIGSe solar cells with an absorber thicknesses of 240, 440, and 670 nm is depicted here, clearly revealing losses close to the band gap that extend more and more toward shorter wavelengths as the absorber thickness decreases. Theoretically, a drop in short-circuit current density j_{SC} of ~7 mA/cm² would be expected, and experimentally we find an even greater loss of 14 mA/cm². This is a clear indication that the ultra-thin absorbers not only suffer from reduced absorption, but also electrical properties become deteriorated, which is confirmed by a drop in open circuit voltage V_{OC} and fill factor. As the absorber thickness is decreased, on the one hand reduced bulk recombination and improved carrier collection can be expected. But once the back contact is within the diffusion length of the photo-generated majority carriers, interface recombination in particular at the back contact can become dominant. The scanning electron microscope (SEM) cross sections in Fig. 2(b) show that good material quality with large grains can still
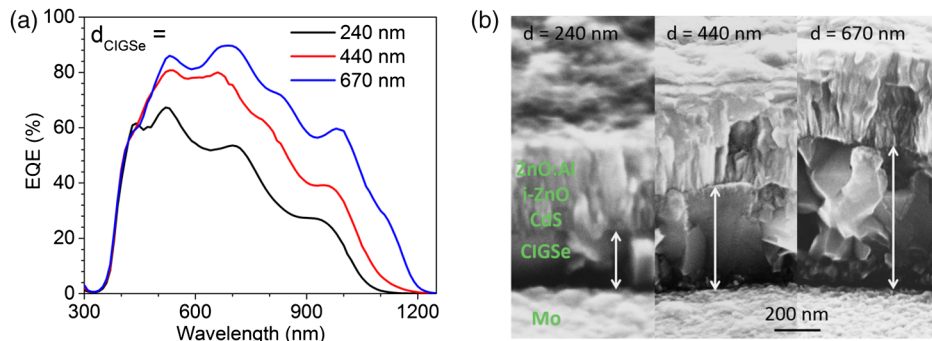
Fig. 2 (a) EQE of thin-film CIGSe solar cells with an absorber thickness of 240, 440, and 670 nm, (b) cross-sectional SEM images of the solar cells with various absorber thicknesses.

be achieved for the ultrathin devices. Nevertheless, the growth process needs to be adapted for ultrathin absorbers and optimized as a function of thickness. Based on a three-stage process optimized for 460 nm absorber thickness with a high back Ga gradient for reducing the back recombination, we could reach at best an efficiency of 11.3%.

The drop in EQE, and hence loss in conversion efficiency of incident photons to extractable current, places at once the dual demands of enhanced absorption and reduced recombination onto the device design. Plasmonic and photonic nanostructures have proven to be effective means for localization of light in ultrathin films. The major effects that can be exploited are scattering of incident light preferentially toward the absorber layer (in the case of plasmonic nanoparticles and a high refractive index absorber), scattering toward large angles and hence enhancement of path length and light trapping in case of total reflection (also mostly for plasmonic nanoparticles), enhancement of electromagnetic field in the direct vicinity of the nanoparticles (near-field enhancement of both plasmonic and photonic nanoparticles), creation of nanojets with high field intensities (by dielectric nano-/microparticles), coupling of light via whispering gallery modes (by dielectric nano-/microparticles) and excitation of waveguide modes redirecting light to propagate inside the absorber layer (by regularly arranged nanoparticles). There are numerous examples of these different effects, and in Ref. 12, we provide a detailed investigation of various configurations of metallic and dielectric nanostructures in ultrathin CIGSe solar cells and their potential for absorption enhancement. As already shown in Ref. 13, dielectric nanostructures are a highly promising alternative to metallic nanoparticles from an optical point of view, and in addition, they provide thermally and chemically stable structures suitable to be deposited prior to a high temperature absorber growth process. The integration of nanostructures at the rear interface has proven most effective for CIGSe solar cells since a direct contact to the absorber layer can be established and any influence on the PN junction avoided.

In Fig. 3, we show results for the absorption of CIGSe solar cells with an absorber thickness of 400 and nanostructures integrated at the CIGSe/Mo interface as simulated using the finite element method (JCMsuite). Two configurations were investigated: hemispherical SiO₂ nanoparticles with a radius of 275 nm and an interparticle spacing of 75 nm in a 2-D hexagonal arrangement as well as the negative of this structure corresponding to a network of SiO₂ obtained by filling the gaps between (inverted hemi-) spheres. The structures are shown in Fig. 3(a), where the shape of the SiO₂ nanostructures and their integration into the absorber layer as well as the other layers of the CIGSe solar cell can be seen. From the absorption of CIGSe given in Fig. 3(b), we can observe a significant increase for wavelengths above 700 nm for both cases of nanostructures as compared with the flat reference. The increase in absorption mainly correlates with a reduction of parasitic absorption in Mo, which is most pronounced for the case of SiO₂ nanoparticles. Figure 3(c) finally shows the electric field distributions at the major resonances (1070 and 1090 nm wavelength, respectively). The near-field pictures reveal that the high electric field intensity is localized in the middle of the absorber layer in the case of nanoparticles and thereby avoids being absorbed in the Mo. For the network, however, the CIGSe nanoparticles emerging within the SiO₂ structure act as cavities localizing the field and giving rise to a high field
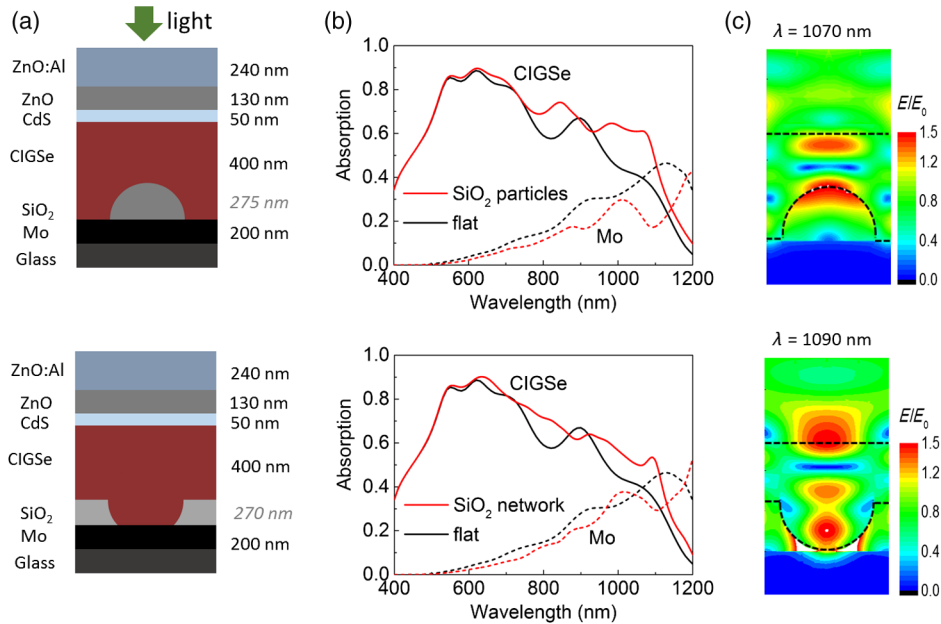
Fig. 3 Simulation of CIGSe solar cells with integrated SiO$_2$ hemispherical nanoparticles (top row) and SiO$_2$ network (bottom row): (a) schematic solar cell structure, (b) calculated absorption of CIGSe and Mo back contact as compared with the flat reference, and (c) electric near-field distribution at the major resonance.

intensity close to the Mo interface. The dielectric network furthermore creates high intensities in the front contact layers (CdS, i-ZnO, ZnO:Al) resulting in parasitic absorption. Thus, despite both SiO$_2$ structures leading to a significant concentration of electromagnetic field inside the absorber layer, the nanoparticles outperform the network in terms of theoretical absorption enhancement. Whereas, the geometry of the nanoparticles already lies in the optimized range (compare Ref. 6), the geometry of the network was assumed as direct negative of the nanoparticle structure for initial comparison. The network dimensions might thus be further optimized to improve light concentration inside the absorber layer. Yet, in any case, a multitude of resonant modes will exist due to the overall large length scales, opening a broad window of suitable parameters. The desired improved reflectivity of the back contact furthermore correlates directly with the overall coverage with low index dielectric, which can particularly be maximized for the network.

In the experiment, where asides optical also electrical influences determine the final performance, the dielectric network turns out highly effective. Figure 4(a) shows an SEM cross section of the experimental realization of integrating an SiO$_2$ network at the Mo/CIGSe interface. The network was obtained via a mask of PS spheres with a diameter of 909 nm, which initially
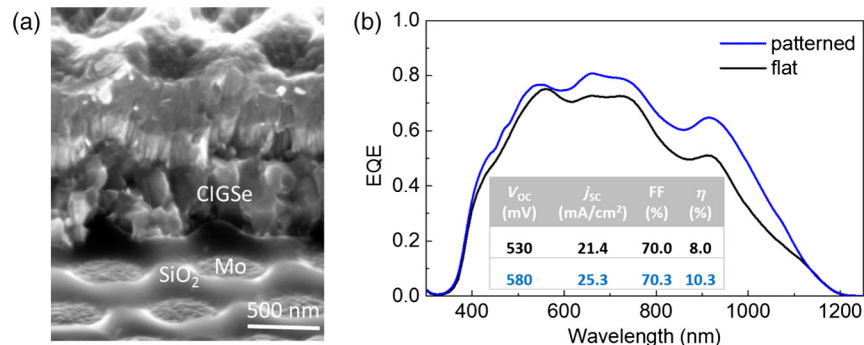

Fig. 4 (a) SEM cross section of an ultrathin CIGSe solar cell on top of an SiO$_2$ network and (b) corresponding EQE as compared with planar reference.

formed a closely packed monolayer and were then reduced to 640 nm in diameter by plasma etching. SiO$_2$ was subsequently deposited onto that mask prior to its removal resulting in the visible free standing network in the front part of the SEM picture. For details of the preparation, see also Ref. 12. The CIGSe absorber and front layers conformally overgrow the network leading to point contacts with the Mo, which is the added electrical benefit of integrating these optically active dielectric nanostructures. The combined optical and electrical benefit of the network can be deduced from the solar cell parameters given as inset in the EQE measurements of Fig. 4(b). The broadband absorption enhancement visible from the EQE reflects an increase in j_{SC} by almost 4 mA/cm^2 related to the optical improvement. In addition, an increase in V_{OC} which is significantly larger than it could be expected from the j_{SC} increase is observed and amounts to 50 mV. The origin can be attributed to the SiO$_2$ network leading to point contacts at the rear interface, thus reducing back contact recombination and improving the carrier collection. The electrical benefits of the network hence add to the optical effects of localizing electric field intensity inside the absorber as expected from the optical simulations shown in Fig. 3(c). An overall increase in efficiency by 29% relative could be achieved.

3 Light Concentration onto Micrometer-Sized Solar Cells

In the second approach of reducing the CIGSe volume, the absorber is restricted in the horizontal dimension. Lamellar and circular structures are possible of which the latter ones enable higher final concentration factors although being more dependent on tracking. The need of direct sunlight for efficient focusing constitutes a substantial requirement of concentrator photovoltaics. A major benefit of the microconcentrators, however, is the facilitation of tracking due to the much more compact devices, which can be fabricated compared with the macroscopic solar concentrator systems. A compactness comparable with thin-film modules opens similar fields of application, supplemented by areas desiring semitransparent modules like building-integrated photovoltaics. Another advantage of micrometer-sized solar cells for operation under concentration is that the small dimensions facilitate heat dissipation. High illumination intensities and related severe heating of the solar cells is addressed in large scale concentrators by (partially active) cooling. On the micrometer scale, heat dissipation across the illuminated absorber area is easily possible, and by adequate choice of substrate material, it can be passively obtained. Therefore, microconcentrator devices combine the benefits of reducing material consumption, exploiting enhanced illumination intensities, and providing compact thin-film devices. A challenge lies in obtaining absorbers of micrometer dimensions.

In Fig. 5, we show examples of circular CIGSe microabsorbers with diameters around 100 to 400 μm. They were obtained by two different approaches: the microabsorber in Fig. 5(a) is a result of top-down processing from a standard planar CIGSe absorber. Therefore, the planar absorber grown in a three-stage coevaporation process was subject to a lithography step, leading to selective coverage by photoresist of the circular area which should remain after etching the surrounding absorber by a piranha solution. The resulting microabsorber shows a relatively sharp edge and a grain structure comparable with the one known for the planar reference. The local absorber obtained by this top-down approach can serve for investigating the performance of micrometer-sized solar cells with absorber quality comparable with the standard device. For true material saving, the microabsorber, however, should not be obtained in a top-down but rather a bottom-up approach. The result of a corresponding bottom-up growth process is
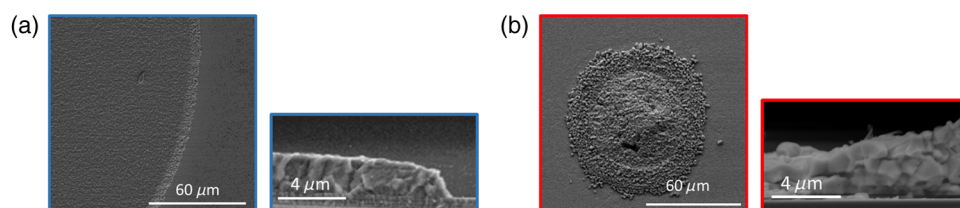

Fig. 5 SEM images of CIGSe microabsorbers fabricated in (a) a top-down and (b) a bottom-up approach.

given in Fig. 5(b). The CISe microabsorber shown here was obtained in a sequential process from In droplets, which were overcoated with Cu and subsequently selenized. For details regarding the preparation of the local In droplets, see Ref. 14. The locally grown absorber reveals a cratered structure with a halo surrounding the central absorber core. A homogeneous distribution of the elements was, however, demonstrated over the entire structure and the cross-sectional image also reveals a granular absorber formation over the entire thickness. The local absorber growth therefore is highly promising for the future realization of micro solar cells fabricated while increasing material conservation.

In Fig. 6, we show the results of electrical measurements of CIGSe microcells sized 400 μm in diameter and obtained in the top-down approach. Figure 6(a) summarizes current–voltage characteristics measured for light intensities ranging from one sun to 30× concentration using a solar simulator with tunable illumination conditions. A clear trend of increasing j_{SC} and V_{OC} can be observed in the given concentration range. The dependence of these parameters on the concentration is shown in Fig. 6(b) up to 80 suns. The linear dependence of j_{SC} can be well reproduced and agrees with theory. V_{OC} is expected to increase logarithmically with concentration, a trend that could equally be confirmed. The fill factor remained almost unaltered (not shown) so that the overall efficiency also improves with the logarithm of the concentration. A maximum efficiency of 11.2% could be obtained at 70× concentration, compared with just 8.0% for no concentration. For even higher illumination intensities, the efficiency started to drop again as heating occurred in the measurements and the solar cells deteriorated. The relatively low efficiency without concentration is a result of decreasing the solar cell size and needs to be tackled in future experiments. From previous investigations, we know that when decreasing the solar cell size, the reduction of initial device efficiency becomes more and more pronounced, yet the stability under high illumination intensities improves, making smaller dimensions favorable.[9,10]

To link the behavior of the microcells under different but spatially homogeneous concentration factors to the realistic concentration distributions emerging by the usage of microlenses, we perform optical ray tracing simulations (Comsol). The investigated lenses were hemispheres with 1 mm radius arranged in a square grid and made from a material of refractive index 1.5. The substrate was made of the same material, whereas light was incident from the opposite side via air (wavelength 543 nm). Figure 7(a) gives the overview of the concentration distribution behind the lens revealing the focusing behavior. Different planes are marked with distances of $L_1 = 1.5$ mm, $L_2 = 1.6$ mm, $L_3 = 1.7$ mm, and $L_4 = 1.8$ mm from the rear of the lens, the latter being closest to the back focal length of 2.0 mm for this configuration.[15] The horizontal dimensions investigated correspond to a spot diameter of 100 μm. In Fig. 7(b), we give the maps of concentration distribution in the planes corresponding to the above distances L_1 to L_4. The local power flow was obtained by summing the power of all rays passing through each individual volume element over time and considering the phase velocity of light passing the lens medium. Concentration factors were then derived by relating to the input power flow of 1000 W/m^2, which corresponds to one sun. An increasing concentration in the center point and a broadening of the main peak are observed as we move closer to the focus. The secondary high concentration
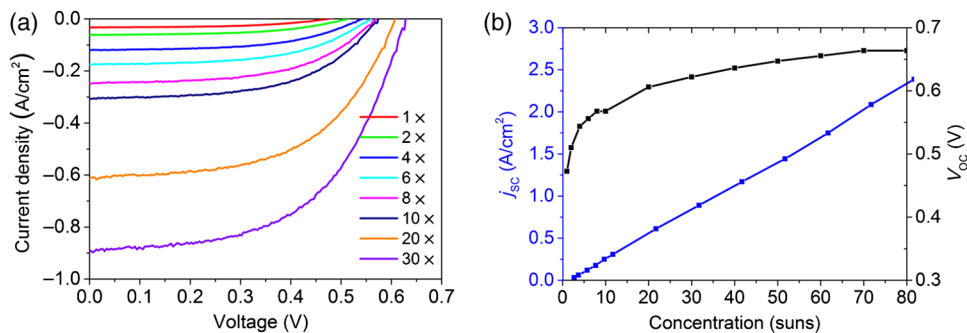

Fig. 6 Electrical measurements of circular CIGSe micro solar cells sized 425 μm in diameter and obtained in a top-down approach: (a) current-voltage characteristics for various concentration factors, (b) j_{SC} and V_{OC} as a function of concentration.
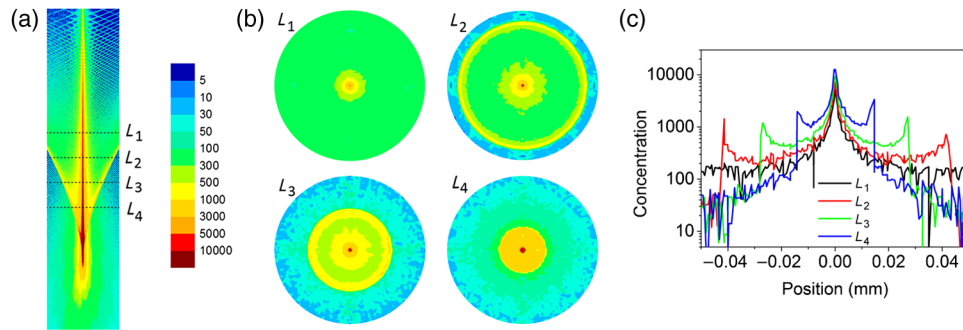
Fig. 7 Optical simulations of hemispherical microlens made from $n = 1.5$ material on such one: (a) ray propagation, lines corresponding to distances of $L_1 = 1.5$ mm, $L_2 = 1.6$ mm, $L_3 = 1.7$ mm, and $L_4 = 1.8$ mm from the lens (not to scale: y-range 1.3 mm, x-range 0.1 mm), (b) concentration distributions in the different planes, spot diameter 100 μm (same color scale as in a), (c) corresponding line profiles through the focal spots.

ring, however, is moving closer to the main peak, leading to an overall decrease of the area where the average highest concentration is found and an increase in lateral concentration variations. A maximum concentration of ~10,000 suns is reached at the center point. These high concentration values could theoretically lead to huge efficiency enhancements, yet they may also be detrimental for the stability of the solar cells. Furthermore, the high concentrations will lead to heating and adequate thermal management is required. In the end, a distance different from the focal plane has to be chosen to provide adequate concentration values and a reasonably homogeneous distribution. Concentration factors exceeding 100 suns and a mostly homogeneous concentration distribution are found for the distance of $L_1 = 1.5$ mm from the lens, i.e., the plane farthest from focus investigated here. Figure 7(c) summarizes the concentration profiles taken through the focal spot for the different planes investigated, which supports the choice of appropriate distance at which to place the micro solar cells. In future considerations, nonimaging optics providing a more uniform lateral concentration distribution should be considered. The averaged concentration factors obtained for the planes L_1 to L_4 are 170×, 262×, 226×, and 189×, respectively. When a laterally homogeneous spread is achieved, these values would be very suitable for application to the micro solar cells.

4 Conclusions

Ultrathin absorbers with a CIGSe thickness of <500 nm offer material saving by a factor of approximately five compared with standard devices. The initial loss in absorption can be well compensated by the integration of dielectric nanostructures, leading to light localization inside the ultrathin absorber. Integration at the rear interface is most beneficial which can additionally enable exploitation of electrical benefits that arise from the formation of point contacts. In this way efficiencies beyond 10% could be achieved for the ultrathin devices. Despite this efficiency achieving only half of the record efficiency, the thickness reduction results in an efficiency per volume increase by a factor of 2.5. For the micrometer-sized solar cells, the material saving factor correlates with the concentration values achieved. In our experimental example, this was above 50; from simulating the focusing behavior of lenses, it could easily be higher. Thus, compared with the ultrathin devices, the material saving can be much higher given that solar cells obtained from locally grown absorbers are available. The reduced efficiencies of micrometer-sized and in particular locally grown solar cells still need to be overcome. Yet, even if only half of the efficiency of the record devices is obtained for the microconcentrator solar cells, due to their huge material saving potential they offer an efficiency increase per volume beyond 25. From a cost perspective, just considering reduced indium consumption, almost 6 €/m² could be saved for micro solar cells under 100× concentration (based on 6 g/m² indium for planar solar cells and costs of 1000 €/kg for high purity material). Microlens arrays with costs as low as 3 €/m², currently found on the market, would leave a net benefit even for this conservative assumption not considering further potential of material saving and efficiency

enhancement. In the future, further work will be required to continuously improve the device configurations and bring them toward the market.

Acknowledgments

References

1. ZSW, "ZSW sets new world record for thin-film solar cells," https://www.zsw-bw.de/en/newsroom/news/news-detail/news/detail/News/zsw-sets-new-world-record-for-thin-film-solar-cells.html (1 July 2016).
2. British Geological Survey, "British Geological Survey: risk list," http://www.bgs.ac.uk/mineralsuk/statistics/risklist.html (1 July 2016).
3. C. Morioka et al., "First flight demonstration of film-laminated InGaP/GaAs and CIGS thin-film solar cells by JAXA's small satellite in LEO," *Prog. Photovoltaics Res. Appl.* **19**(7), 825–833 (2011).
4. H. A. Atwater and A. Polman, "Plasmonics for improved photovoltaic devices," *Nat. Mater.* **9**, 205–213 (2010).
5. M. Gu et al., "Nanoplasmonics: a frontier of photovoltaic solar cells," *Nanophotonics* **1**(3–4), 235–248 (2012).
6. C. van Lare et al., "Light coupling and trapping in ultrathin Cu(In, Ga)Se$_2$ solar cells using dielectric scattering patterns," *ACS Nano* **9**(10), 9603–9613 (2015).
7. G. Yin, P. Manley, and M. Schmid, "Light absorption enhancement for ultra-thin Cu(In$_{1-x}$, Ga$_x$)Se$_2$ solar cells using closely packed 2-D SiO$_2$ nanosphere arrays," *Sol. Energy Mater. Sol. Cells* **153**, 124–130 (2016).
8. J. Yoon et al., "Ultrathin silicon solar microcells for semitransparent, mechanically flexible and microconcentrator module designs," *Nat. Mater.* **7**(11), 907–915 (2008).
9. M. Paire et al., "Physics of Cu(In, Ga)Se$_2$ microcells under ultrahigh illumination intensities," *Proc. SPIE* **8620**, 86200Z (2013).
10. B. Reinhold et al., "Monolithically interconnected lamellar Cu(In, Ga)Se$_2$ micro solar cells under full white light concentration," *Prog. Photovoltaics Res. Appl.* **23**(12), 1929–1939 (2015).
11. T. Negami et al., "Effect of absorber thickness on performance of Cu(In, Ga)Se$_2$ solar cells," in *Proc. 2nd World Conf. and Exhibition on Photovoltaic Solar Energy Conversion*, Vienna, Austria, pp. 1181–1184 (1998).
12. M. Schmid et al., "Nanoparticles for light management in ultra-thin chalcopyrite solar cells," *J. Mater. Res.* **31**, 3273–3289 (2016).
13. M. Schmid, P. Andrae, and P. Manley, "Plasmonic and photonic scattering and near fields of nanoparticles," *Nanoscale Res. Lett.* **9**, 50 (2014).
14. F. Ringleb et al., "Regularly arranged indium islands on glass/molybdenum substrates upon femtosecond laser and physical vapor deposition processing," *Appl. Phys. Lett.* **108**(11), 111904 (2016).
15. M. Schmid and P. Manley, "Nano- and microlenses as concepts for enhanced performance of solar cells," *J. Photonics Energy* **5**(1), 057003 (2014).

Biographies for the authors are not available.